arXiv:1510.05834v1 [quant-ph] 20 Oct 2015

Superfluid-Mott transitions and vortices in the Jaynes-Cummings-Hubbard lattices with time reversal symmetry breaking

A.L.C. Hayward[1] and A.M. Martin[1]

[1]*School of Physics, University of Melbourne, Victoria 3010, Australia*

(Dated: October 21, 2015)

We investigate the groundstate behaviour of Jaynes-Cummings-Hubbard lattices in the presence of a synthetic magnetic field, via a Gutzwiller ansatz. Specifically, we study the Mott-Superfluid transition, and the formation of vortex lattices in the superfluid regime. We find a suppression of the superfluid fraction due to the frustration induced by the incommensurate magnetic and spacial lattice lengths. We also predict the formation of triangular vortex lattices inside the superfluid regime.

PACS numbers: 67.80.K-, 67.80.kb, 42.50.Pq, 32.80.Qk

A Jaynes-Cummings Hubbard (JCH) lattice [1–3] consists of an array of coupled photonic cavities, with each cavity mode coupled to a two-level atom [Figs. 1 (a) and 1(b)]. The JCH model is predicted to exhibit a number of solid state phenomena, including Mott and superfluid phases [2], supersolid phases [4], semiconductor physics [5] Josephson effect [6], metamaterial properties [7], and Bose-glass phases [8] and, in the presence of synthetic magnetic fields, fractional quantum Hall states [9].

In this paper we examine how the introduction of a synthetic magnetic field affects the superfluid Mott insulator phase transition and leads to the formation of vortices in the superfluid phase. In section I we introduce the formalism and numerical techniques under which we will study the JCH model. Section II examines the properties of the phase transition, and how the presence of a synthetic magnetic field affects the Mott-superfluid transition. Our results suggest that frustration due to incommensurate magnetic/spacial lattices suppresses the emergence of a superfluid phase at strong non-linear interaction strengths. Finally, in section III, we study the formation of vortices in the photonic field in the superfluid regime. We find that vortices in the photonic field of the JCH behave in a similar way to those found in continuous superfluids, including the formation of a triangular Abrikosov lattice.

I. JAYNES-CUMMINGS-HUBBARD MODEL

Each cavity [Fig. 1(b)] in the JCH lattice is described by the Jaynes-Cummings (JC) Hamiltonian ($\hbar = 1$)

$$H^{\mathrm{JC}} = \omega L + \Delta\sigma^{+}\sigma^{-} + \beta\left(\sigma^{+}a + \sigma^{-}a^{\dagger}\right), \qquad (1)$$

where a is the photonic annihilation operator, $\sigma^{\pm}$ are the atom raising and lowering operators, Δ is the atom-photon detuning and β is the coupling energy. For n photons the state $|g(e), n\rangle$ forms the single cavity basis, where $g(e)$ denote the ground (excited) state of the atom.

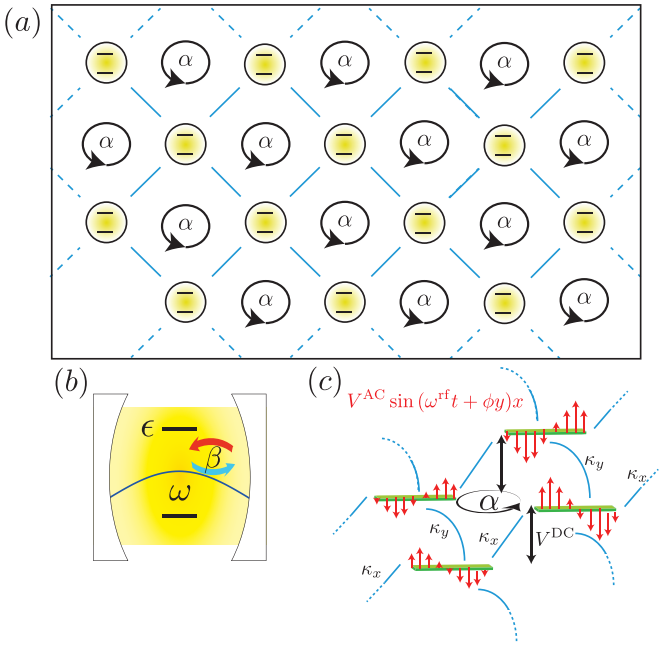

FIG. 1: (color online). (a) Schematic of a square JCH lattice with a constant synthetic magnetic field. Photons moving around a plaquette acquire a phase $2\pi\alpha$ (b) A single-mode photonic cavity with frequency ω coupled to a two-level atom with strength β. (c) Scheme for breaking time reversal symmetry in photonic cavities: a potential $V = \left[V^{\mathrm{DC}} + V^{\mathrm{AC}}\sin\left(\omega^{\mathrm{rf}} + 2\pi\alpha y\right)\right]x$, where x and y are in units of the lattice spacing, is applied to the cavities by dynamically tuning ω. The phase offset, $2\pi\alpha$, along y results in the synthetic magnetic field seen in (a).

Throughout this paper we shall be using the dressed basis

$$|\pm, \ell\rangle = \frac{\beta\sqrt{\ell}|g, \ell\rangle + [-\Delta/2 \pm \chi]\,|e, \ell - 1\rangle}{\sqrt{2\xi^2 \mp \xi\Delta}}, \qquad (2)$$

with

$$\chi = \sqrt{\ell\beta^2 + \Delta^2/4} \qquad (3)$$

the generalized Rabi frequency, and ℓ refers to the total number of excitations in the cavity. In this basis the

energy of a single cavity, with ℓ excitations is

$$E_{\pm,\ell} = \ell\omega \pm \chi - \Delta/2. \tag{4}$$

Since $H^{\rm JC}$ commutes with the total excitation number operator, $L = a^\dagger a + \sigma^+\sigma^-$ the total excitations in the cavity, ℓ, is a good quantum number. The eigenstates of Eq. (1) are termed polaritons, superpositions of atomic and photonic excitations, and are a function of ℓ and Δ/β.

The JCH model describes a tight-binding JC lattice [Fig. 1(a) with $\alpha = 0$]:

$$H^{\rm JCH} = H^{\rm JC} + K = \sum_i^N H_i^{\rm JC} - \sum_{\langle i,j\rangle} \kappa_{ij} a_i^\dagger a_j, \tag{5}$$

where κ_{ij} is the photon tunnelling rate between cavities i and j and the sum over $\langle i,j\rangle$ is between nearest neighbours only.

Exact solutions to $H^{\rm JCH}$ are know in two limits; $\kappa/\beta \to 0$, and $\beta/\kappa \to 0$. In the former limit, each cavity is decoupled, and the eigenstates are simply product states of individual cavities, described by the solutions in Eq. (2). In the opposite limit, where $\beta/\kappa \to 0$, the photonic and atomic degrees of freedom decouple. This removes the non-linearity from the photonic field, and any interatomic coupling, again reducing the eigenstates to product states of single-particle.

A. The Gutzwiller Ansatz

For large system sizes, the exact quantum mechanical problem of the JCH model is too computationally difficult to approach directly, either analytically or numerically. Various approximations have been used to study the superfluid Mott insulator phase transition in the JCH model [2, 10]. In this paper we use a Gutzwiller ansatz to study the JCH groundstate wavefunction. The Gutzwiller ansatz imposes a trial wavefunction that is a product state of individual lattice sites:

$$P_\ell |\Psi^{\rm GW}\rangle = \prod_i^{\rm sites} |\psi_i\rangle \tag{6}$$

where P_ℓ projects onto an excitation number eigenstate. Applying $|\Psi^{\rm GW}\rangle$ to the JCH Hamiltonian yields an effective Hamiltonian that is a sum over single cavity Hamiltonians:

$$H_{\rm eff}^{\rm JCH} = \sum_i^N H_i^{\rm JC} - \sum_{\langle i,j\rangle} \left[\kappa_{ij}\psi_j^\star \left(a_i - \frac{1}{2}\psi_i \right) + \text{h.c.} \right], \tag{7}$$

where we have introduced the notation $\psi_i = \langle\psi_i|a_i|\psi_i\rangle$. With this effective Hamiltonian in hand, the Gutzwiller groundstate can be found by minimising the energy of $H_{\rm eff}^{\rm JCH}$.

The local superfluid order parameter $\vec{\psi} = \{\psi_i\}$ determines the nature of the groundstate. From Eq. (7) it follows that the off diagonal elements of the single particle density matrix are determined by $\vec{\psi}$: $\rho_{ij}^1 = \psi_i\psi_j^\star$. The system can be said to be superfluid whenever there are system wide connected non-zero ψ_i's. The Mott insulating phase is characterised by $\psi_i = 0$ across the whole system.

The effective Hamiltonian arrived at though the Gutzwiller procedure removes the restriction of the system to a specific number of excitations, since, except in the $\vec{\psi} = 0$ case, the Hamiltonian does not conserve the particle number. However, it is possible to restrict the particle density implicitly though the introduction of a chemical potential:

$$H = H^{\rm JCH} - \mu L. \tag{8}$$

That is, the system is now studied in the grand-canonical ensemble, and the system's groundstate at the desired density is found by varying the chemical potential. In the case of the effective Hamiltonian in Eq. (7), this is necessary, since this Hamiltonian does not preserve photon number.

There has been some confusion in the literature[2, 11] as to the physical significance, or meaning, of the chemical potential in photonic systems. From a mathematical perspective, the chemical potential introduced in this manner acts simply as a Lagrange multiplier. The choice of μ defines an excitation density for the groundstate. The chemical potential can also appear as a real physical quantity. Consider the JCH weakly coupled to a bath of photons, all with frequency ω_b such that $\omega - \omega_b = \mu$. Assuming a mechanism for thermalization, such a coupling of the bath to atomic or photonic modes, the pump will act to drive the system to some groundstate, determined by $\mu = \omega_{pump}$. Weakly blue band pumping will act to create a positive chemical potential for photons in the system. Although a JCH system under such pumping, when paired with photon losses, will exhibit non-equilibrium dynamics, when these effects are small, the system will be well described by Eq. (8) in the groundstate[12].

For real world cavity lattices, the photons in the system will not be conserved, due to dissipation. In contrast to cold atom systems, where some set number of particles can be loaded into the lattice, a photonic lattice is driven by a laser, and will be in a steady state where losses and driving equilibrate[13]. Still, for an array of high quality cavities, one may consider a regime of weak pumping, and weak losses, such that the mean-field approximation made here captures the broad physics of the system[14].

B. Synthetic Magnetic Field

An artificial magnetic field may be realized via the introduction of some time reversal symmetry breaking interaction. A number of techniques have been proposed

to achieve this[15–17]. For example, one may exploit a time-dependent potential to induce magnetic flux across the lattice (as in Fig 1(c))[16].

Defining the magnetic field by a vector potential $\mathbf{A}(x)$ results in minimal substitution, $\mathbf{p} \to \mathbf{p} - q\mathbf{A}(x)$. On a tight-binding lattice, a vector potential $\mathbf{A}$ manifests as a complex hopping rate $\kappa_{ij} \to \kappa_{ij} e^{i2\pi\theta_{ij}}$, where $2\pi\theta_{ij} = \int_{r_i}^{r_j} \mathbf{A}(r)dr$. Gauge symmetry implies that the only physically important parameter is the total phase, $2\pi\alpha$, picked up around a closed loop, where $\alpha = \Phi/\Phi_0$ is the fraction of flux quanta through the loop. A uniform magnetic field through the two dimensional lattice corresponds to a constant α for all plaquettes on the lattice. Factors of 2π in the phase around a loop are physically inconsequential, so we only need consider $\alpha \in [0, 1)$.

II. PHASE DIAGRAM

The simplest situation in which the Mott-superfluid transition occurs is in the homogeneous lattice, with $\alpha = 0$. Since the meanfield ground state of our Hamiltonian is invariant under translations along lattice vectors it is possible to significantly simplify the problem to that of a single site. That is, since $|\psi_i\rangle = |\psi_j\rangle \forall i, j$ we have just a single $\psi = \langle a_i \rangle$ that characterises the whole ground-state. Hence for $\alpha = 0$ we find the well-known result[1–3] [Fig. 2(a)] that the parameter space is separated into two distinct phases. For low hopping strength $\overline{\kappa} = \kappa/\beta$, we find lobes of vanishing superfluid order parameter, i.e., Mott-insulating phases as shown in Fig. 2(a). Each lobe corresponds to a state with an integer number of strongly localised excitations per site. For example the first (second) Mott lobe, with $\overline{\mu} = (\mu - \omega)/\beta < -1$ ($-1 < \overline{\mu} = (\mu - \omega)/\beta < -0.4$) corresponds to the states $|-, 0\rangle$ ($|-, 1\rangle$). For low chemical potential, there are no excitations in the system. Raising the chemical potential, the block is successively filled with one, two, and more excitations per site. At sufficiently large $\overline{\kappa}$, the system undergoes a phase transition into a phase of finite superfluid order parameter [Fig. 2(a)]. The excitations are homogeneously distributed and delocalised, i.e., the system is in a superfluid state.

The Mott-superfluid transition in the JCH lattice is now considered in the presence of a synthetic magnetic field $\alpha \neq 0$. This situation differs in several key ways from the non-magnetic case. Specifically, the field introduces a *magnetic lattice* which breaks the translational symmetry of the underlying lattice. Hence, with a magnetic field, ψ_i's can not be assumed identical across the system. To capture this, a large lattice must be simulated, so that the magnetic and cavity lattices are commensurate. For the magnetic parameter $\alpha = p/q$, there must be $q = N_x \times N_y$ sites, where N_x (N_y) is the number of cavities along the x (y) axis. Despite this introducing a synthetic magnetic field does not qualitatively change the

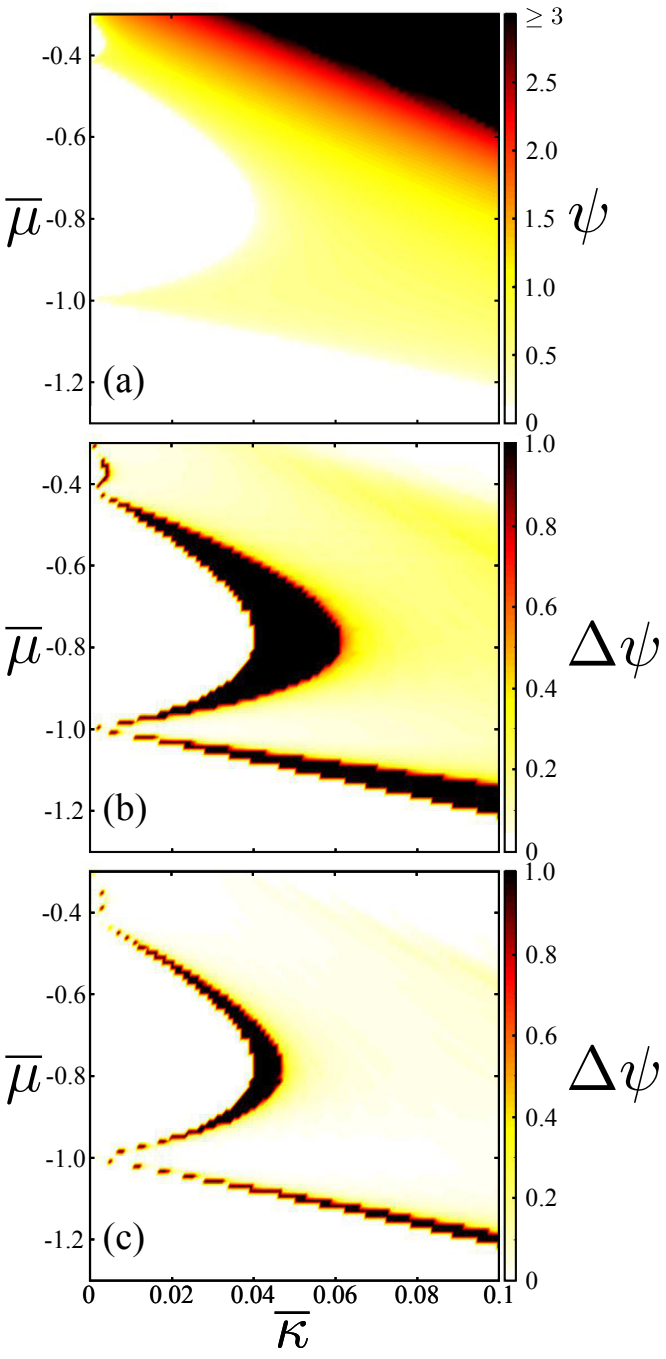

FIG. 2: (color online). (a) The superfluid order parameter (ψ) as a function of the chemical potential $\overline{\mu}$ and the interactive hopping $\overline{\kappa}$, with a lattice of 4×5 sites in the absence of synthetic magnetic field ($\alpha = 0$). (b,c) $\Delta\psi$ as a function of the chemical potential $\overline{\mu}$ and the interactive hopping $\overline{\kappa}$, for $|\alpha| = 2/5$ and $3/5$. (b) and $|\alpha| = 1/10$ and $9/10$. (c), with $\epsilon = 0.001$. For (a-c) we have introduced the following dimensionless parameterisation: $\overline{\kappa} = \kappa/\beta$, $\overline{\mu} = (\mu - \omega)/\beta$ and $\overline{\Delta} = \Delta/\beta = 0$

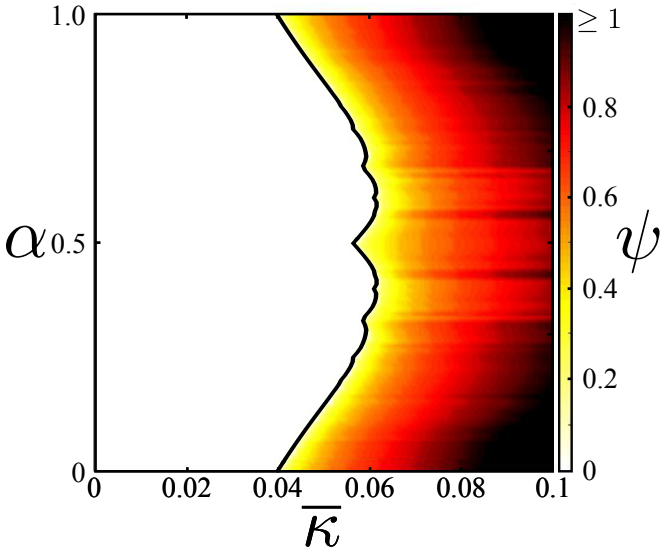

FIG. 3: (color online). The maximum superfluid order parameter ($\max[\vec{\psi}]$) as a function of the synthetic magnetic field α and the interactive hopping $\overline{\kappa}$, with $\overline{\mu} = -0.78$ for a 20×20 lattice. The solid black curve corresponds to the evaluation of the transition between the Mott insulator state and the superfluid state as determined by Eq. (14). We have introduced the following dimensionless parameterisation: $\overline{\kappa} = \kappa/\beta$, $\overline{\mu} = (\mu - \omega)/\beta$ and $\overline{\Delta} = (\omega - \epsilon)/\beta = 0$

phase diagram for the Mott-insulator superfluid phase transition, i.e. at low $\overline{\kappa}$ the lobe structure persists and when $\overline{\kappa}$ is sufficiently large the system undergoes a transition to superfluid state. However, the introduction of a synthetic magnetic field does quantitatively change the phase diagram, see Figs. 2(b,c). Here, we compare the superfluid density at non-zero α to the $\alpha = 0$ case (at some μ and κ)via

$$\Delta\psi(\alpha) = \frac{\max[\vec{\psi}(\alpha=0)] - \max[\vec{\psi}(\alpha)]}{\max[\vec{\psi}(\alpha=0)] + \max[\vec{\psi}(\alpha)] + \epsilon}, \qquad (9)$$

where we have introduced ϵ to avoid divide by zero errors, but which plays no physical role. Specifically we see that the introduction of a synthetic magnetic field changes (for a fixed chemical potential) the strength of inter-cavity hopping required to transition from the Mott-phase to the superfluid phase.

To quantify how the synthetic magnetic field changes the boundary between the superfluid and Mott phase in Fig. 2 we have plotted, in Fig. 3, $\max[\vec{\psi}]$ as a function of $\overline{\kappa}$ and α, with $\overline{\mu} = -0.78$. This shows that increasing the synthetic magnetic field from zero (half a) flux quanta per site to half a (one) flux quanta per site the superfluid Mott insulator boundary is pushed to larger (lower) values of the inter-cavity hopping.

In the vicinity of the Mott insulator superfluid phase boundary the superfluid parameters ψ_i are very small across the entire system. Perturbatively expanding about ψ_i it is possible to determine the boundary between the superfluid and Mott phases. Specifically, consider the single site effective Hamiltonian for site i

$$H^{\rm JCH}_{{\rm eff},i} = H^{\rm JC}_i - \mu L_i - \kappa \sum_j \left[\left(a_i^\dagger - \frac{1}{2}\psi_i^\star \right) \Psi_i + {\rm h.c.} \right], \qquad (10)$$

where $\Psi_i = \sum_j \kappa_{ij}\psi_j/\kappa$ and we have assumed that the magnitude of the hopping rate is the same between sites, i.e. $|\kappa_{ij}| = \kappa$. Treating the ψ_i's as perturbative parameters we find

$$E_i(\vec{\psi}) \;=\; E_i^{(0)} - r_n\kappa^2 \left|\Psi_i\right|^2 - \frac{\kappa}{2}\left(\psi_i^\star \Psi_i + {\rm h.c.}\right), \qquad (11)$$

where

$$r_n = \sum_{\gamma=\pm} \frac{\left|\langle \gamma, n+1 \left| a \right| -, n\rangle\right|^2}{E_{n+1,\gamma} - E_{n,-} - \mu} + \frac{\left|\langle \gamma, n-1 \left| a \right| -, n\rangle\right|^2}{E_{n-1,\gamma} - E_{n,-} - \mu} \qquad (12)$$

arises from the second order perturbative corrections to the energy. The full energy can then be written as

$$E(\vec{\psi}) = \sum_i E_i^{(0)} + \kappa\vec{\psi}^\dagger \boldsymbol{\kappa}(\alpha)\vec{\psi} - r_n\kappa^2\vec{\psi}^\dagger\boldsymbol{\kappa}^2(\alpha)\vec{\psi}, \qquad (13)$$

where $\vec{\psi}$ is a vector of the ψ_i's and the elements of the matrix $\boldsymbol{\kappa}$ parameterise the phase accumulated, due to the synthetic magnetic field, in hopping between sites. The location of the Mott insulator superfluid transition occurs when some non-zero values for ψ_i gives an energy lower than the energy of the Mott lobe, i.e.

$$\kappa\vec{\psi}^\dagger\boldsymbol{\kappa}\vec{\psi} - r_n\kappa^2\vec{\psi}^\dagger\boldsymbol{\kappa}^2\vec{\psi} < 0. \qquad (14)$$

The solid line in Fig. 3 shows how the phase boundary between the Mott insulator and superfluid changes as a function of the hopping and α, as determined from the above equation. As expected, we find very good agreement between this perturbative calculation and the full mean-field calculation in determining the boundary between the two regimes.

The solutions for Eq.(14) occur for $\kappa > 1/\kappa f(\alpha)$, where $f(\alpha)$ is the maximum eigenvalue of $\boldsymbol{\kappa}(\alpha)$. As noted in studies of the Bose-Hubbard model[18], $f(\alpha)$ is the outline of the Hofstadter butterfly. Thus the suppression of the phase transition comes from the frustration induced by the incommensurate lattice/magnetic lengths. This leads in general to fractal structures (as seen in the Hofstadter Butterfly), and is similarly reflected in the phase boundary seen here.

In Fig. 3 we note that the some of the very fine structure in $f(\alpha)$ is visible, both in the location of the boundary, and within the superfluid region. This structure is perhaps over represented in the figure since, in finding the groundstate wavefunction, we limited the system size to a 20×20 lattice. The presence of butterfly like structure has already been observed in experiments[19, 20],

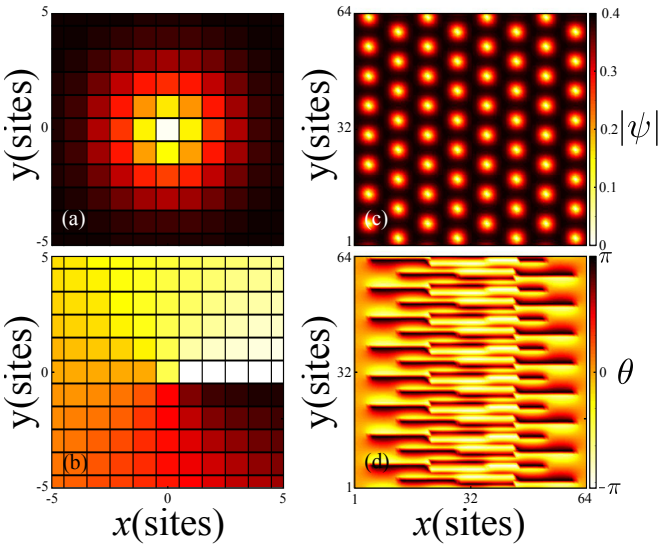

FIG. 4: (color online). Superfluid density $|\psi|$ (a,c) and phase (b,d) on a 64×64 lattice, with $\overline{\kappa} = 0.045$, $\overline{\Delta} = 0$ and $\overline{\mu} = -0.78$ for $\alpha = 1/64^2$ (a,b) and $\alpha = 1/64$ (c,d).

including some involving photons[21]. As expected[22], small fluctuations in the system lead to a blurring of the fractal structure, and so the very fine structure seen in Fig. 3 would be challenging to resolve in any experiment.

III. VORTICES

In dilute Bose gas superfluids the introduction of synthetic magnetic fields[23–27], or the application of rotation to break time reversal symmetry, has lead to the observation of single vortices[28], vortex lattices[29–31], and the prediction of the emergence of fractional quantum Hall states[23, 32–37]. The application of a synthetic magnetic field in a JCH lattice is expected to produce similar effects in the superfluid state. Considerable effort has already been applied to the study of of fractional quantum Hall states[8] in the 'high' synthetic magnetic field regime, where the number of flux quanta though the lattice is larger than the number of excitations. However, less attention has been paid to the emergence of a vortex and vortex lattice states in the 'low' synthetic magnetic field regime. Below we demonstrate that the JCH system does admit vortex and vortex lattice solutions in the superfluid regime, upon the introduction of a synthetic magnetic field.

In the context of the meanfield description of JCH model, the local order parameter shares all the characteristics of a superfluid. Figures 4(a,b) show the magnitude of the mean field order parameter (a) and its phase (b) for a periodic lattice with a single flux quantum penetrating 64×64 sites. Minimizing the meanfield energy functional(Eq. 11) results in a single vortex structure where the superfluid density rises monotonically from the centre of the vortex core and the superfluid phase rotates by 2π.

At higher synthetic magnetic fields one expects multiple vortices to be admitted into the superfluid. In the absence of an underlying lattice structure the vortices will arrange themselves into a triangular Abrikosov vortex lattice. This configuration arises, in the presence of a local repulsive non-linearity, to minimize the self-interaction of the superfluid at a given density of vortices. Figures 4(c,d) show that energy minimization of the meanfield JCH, in the presence of a synthetic magnetic field, also leads to the formation of an Abrikosov vortex lattice state.

IV. CONCLUSIONS

We have shown that the introduction of a synthetic magnetic field to the JCH model modifies the boundary between the Mott-Insulator and superfluid regimes. This modification arises from a competition between the magnetic lattice and the spatial lattice. Additionally, we predict that in the superfluid regime the introduction of a synthetic magnetic field leads to the formation of vortices which, due to the local non-linear atom-photon interaction, forms a triangular lattice in the groundstate.

This work opens up possible avenues for future research into the role of the JCH atom-cavity interaction in frustrating the formation of triangular Abrikosov vortex lattices, and, since this is an inherently two dimensional system, the possibility of observing a BKT transition.

[1] M. J. Hartmann, F. G. S. L. Brandão, and M. B. Plenio, Nature Physics **2**, 849 (2006), ISSN 1745-2473.

[2] A. D. Greentree, C. Tahan, J. H. Cole, and L. C. L. Hollenberg, Nature Physics **2**, 856 (2006), ISSN 1745-2473.

[3] D. Angelakis, M. Santos, and S. Bose, Physical Review A **76** (2007), ISSN 1050-2947.

[4] B. Bujnowski, J. K. Corso, A. L. C. Hayward, J. H. Cole, and A. M. Martin, Physical Review A **90**, 043801 (2014), ISSN 1050-2947.

[5] J. Quach, M. I. Makin, C.-H. Su, A. D. Greentree, and L. C. L. Hollenberg, Physical Review A **80** (2009), ISSN 1050-2947.

[6] D. Gerace, H. E. Türeci, A. Imamoglu, V. Giovannetti, and R. Fazio, Nature Physics **5**, 281 (2009), ISSN 1745-2473.

[7] J. Q. Quach, C.-H. Su, A. M. Martin, A. D. Greentree, and L. C. L. Hollenberg, Optics express **19**, 11018 (2011), ISSN 1094-4087.

[8] E. Kapit, M. Hafezi, and S. H. Simon, Physical Review X **4**, 1 (2014), ISSN 2160-3308, arXiv:1402.6847v1.

[9] D. Rossini and R. Fazio, Physical Review Letters **99** (2007), ISSN 0031-9007.

[10] M. Hohenadler, M. Aichhorn, S. Schmidt, and L. Pollet, Physical Review A **84** (2011), ISSN 1050-2947.

[11] H. Zheng and Y. Takada, Physical Review A **84**, 043819 (2011), ISSN 1050-2947.

[12] A. Hu, T. E. Lee, and C. W. Clark, Physical Review A **88**, 053627 (2013), ISSN 1050-2947.

[13] I. Carusotto and C. Ciuti, Reviews of Modern Physics **85**, 299 (2013), ISSN 0034-6861.

[14] A. Le Boité, G. Orso, and C. Ciuti, Physical Review A **90**, 063821 (2014), ISSN 1050-2947.

[15] J. Koch, A. Houck, K. L. Hur, and S. Girvin, Physical Review A **82** (2010), ISSN 1050-2947.

[16] A. R. Kolovsky, EPL (Europhysics Letters) **93**, 20003 (2011), ISSN 0295-5075.

[17] R. O. Umucalilar and I. Carusotto (2011), 1104.4071.

[18] M. Oktel, M. Ni, and B. Tanatar, Physical Review B **75** (2007), ISSN 1098-0121.

[19] C. R. Dean, L. Wang, P. Maher, C. Forsythe, F. Ghahari, Y. Gao, J. Katoch, M. Ishigami, P. Moon, M. Koshino, et al., Nature **497**, 598 (2013), ISSN 1476-4687.

[20] T. Schlösser, K. Ensslin, J. P. Kotthaus, and M. Holland, Europhysics Letters (EPL) **33**, 683 (1996), ISSN 0295-5075.

[21] U. Kuhl and H.-J. Stöckmann, Physical Review Letters **80**, 3232 (1998), ISSN 0031-9007.

[22] D. Hofstadter, Physical Review B **14**, 2239 (1976), ISSN 0556-2805.

[23] J. Ruostekoski, G. V. Dunne, and J. Javanainen, Physical Review Letters **88**, 180401 (2002), ISSN 0031-9007.

[24] D. Jaksch and P. Zoller, New Journal of Physics **5**, 56 (2003), ISSN 1367-2630.

[25] E. J. Mueller, Physical Review A - Atomic, Molecular, and Optical Physics **70**, 1 (2004), ISSN 10502947, 0404306.

[26] I. B. Spielman, Physical Review A - Atomic, Molecular, and Optical Physics **79**, 1 (2009), ISSN 10502947, 0905.2436.

[27] D. R. Murray, P. Öhberg, D. Gomila, and S. M. Barnett, Physical Review A - Atomic, Molecular, and Optical Physics **79**, 1 (2009), ISSN 10502947.

[28] Y.-J. Lin, R. L. Compton, K. Jiménez-García, J. V. Porto, and I. B. Spielman, Nature **462**, 628 (2009), ISSN 1476-4687.

[29] K. Madison, F. Chevy, and W. Wohlleben, Physical review letters **84**, 806 (2000), ISSN 1094-5695, 9912015.

[30] K. W. Madison, F. Chevy, V. Bretin, and J. Dalibard, Physical Review Letters **86**, 4443 (2001), ISSN 00319007, 0101051.

[31] E. Hodby, G. Hechenblaikner, S. A. Hopkins, O. M. Maragò, and C. J. Foot, Physical Review Letters **88**, 010405 (2001), ISSN 0031-9007.

[32] N. Cooper and N. Wilkin, Physical Review B **60**, R16279 (1999), ISSN 0163-1829.

[33] N. K. Wilkin and J. M. F. Gunn, Physical Review Letters **84**, 6 (2000), ISSN 0031-9007.

[34] N. Cooper, N. Wilkin, and J. Gunn, Physical Review Letters **87**, 120405 (2001), ISSN 0031-9007.

[35] V. Bretin, S. Stock, Y. Seurin, and J. Dalibard, Physical Review Letters **92**, 050403 (2004), ISSN 0031-9007.

[36] V. Schweikhard, I. Coddington, P. Engels, V. P. Mogendorff, and E. A. Cornell, Physical Review Letters **92**, 040404 (2004), ISSN 0031-9007.

[37] M. A. Baranov, K. Osterloh, and M. Lewenstein, Physical Review Letters **94**, 070404 (2005), ISSN 0031-9007.